

Investigation of the Effects of Nozzle Exit Mach Number and Nozzle Pressure Ratio on Axisymmetric Flow through Suddenly Expanded Nozzles

Sher Afghan Khan, M. Mohiuddin, Ahmad Saleel C., Fharukh G. M.

ABSTRACT--- *Computational Fluid Dynamics simulations were carried out using ANSYS FLUENT for suddenly expanded flow through the convergent-divergent nozzle and a suddenly expanded duct. The Length-to-Diameter ratio of 10 for the duct was used in the analysis. Also, an Area Ratio between CD Nozzle exit area and Duct Area was used to be 1.6. The effects of Nozzle Exit Mach number and the Nozzle Pressure Ratios were evaluated by conducting the simulations for Nozzle Exit Mach numbers: 1.87, 2.25 and 2.58. For each Mach number then, Nozzle Pressure Ratios of 3, 5, 7, 9, and 11 were set respectively. Making a total of 15 cases. All the cases were simulated using the k- ω turbulence model. Simulated results agree with the experimental data. From the analysis, it is clear that the Nozzle Exit Mach number and Nozzle Pressure Ratio have a direct effect on the expanded flow exiting the nozzle.*

Index Term— *Base Pressure; Wall Pressure; Flow Characteristics; Nozzle Pressure Ratio.*

I. INTRODUCTION

The investigation of suddenly expanded flow has implementations in numerous territories. With the necessity to procure rockets, and scramjets to meet the future financial prerequisites, the outlines of the nozzles must be looked into further. In need for recently developed and future nozzle designs for propulsion systems, the execution and results improve alongside the reduction of cost, which is apparently the most reassuring issue. As the flow suddenly expands, suction zones are created at the base of the duct. The pressure is generally less in the base region in comparison to atmospheric pressure. It is thus necessary to outline the extended duct and select legitimate geometrical parameters that produce better usage [8]. The pressure created after this sudden expansion is known as base drag. Base drag is the

kind of pressure drag that overwhelms at excessive speeds and makes a zone of vacuum after the bluff bodies [10]. As the occurrence of separation is predominant at higher Mach numbers, different sorts of loads occur in the presence of dynamic conditions. Wall pressure effect on the analysis of flow is one such occurrence. Hence, wall pressure influences flow performance [11]. The wall pressure data can also predict the reattachment length and dictate the formation of suction zones. Nozzle Exit Mach number can be defined as the Mach number of the flow leaving the exit of the convergent, divergent nozzle. Isentropic flow tables can be used to calculate this Mach number for a specific convergent-divergent nozzle design. On the other hand, The Nozzle Pressure Ratio (NPR) is the ratio of stagnation pressure in the settling chamber to the environmental pressure when the jet is exhausted. NPR identifies the extent of flow expansion at the nozzle exit. The jet is termed as over-expanded when the static pressure at the nozzle exit is less than environment pressure. For the situation when the exit pressure is equal to the environmental pressure, the jet is said to be correctly expanded and the case when the exit pressure is larger than the pressure in the environment, the jet is termed as under-expanded. In the cases of under-expansion, expansion fan is found, and for over-expanded flows, oblique shocks at the nozzle throat are found [4]. Many turbulence models may be used to analyze the flow but the standard k- ω model is used. The k- ω turbulence model, developed by Wilcox [3] has exhibited the best results in different applications. The wall-resolved standard k- ω model does not employ damping functions and has a formulation with straightforward Dirichlet boundary conditions that lead to significant advantages in numerical stability [2]. The standard k- ω model considers the effect of low Reynolds number; it can be calculated directly to the wall. Therefore, the standard k- ω model could obtain more reasonable results for simulating the flow near the wall compared to the standard k- ϵ model [2]. Assuming the air to be an ideal gas, the investigation, and analysis conducted in this paper involves the use of k- ω turbulence model to study the effects of increments in NPR and Nozzle exit Mach numbers on the suddenly expanded flow. NPR's 3, 5, 7, 9, 11 and models for nozzle exit Mach numbers 1.87, 2.2 and 2.58 are used.

Manuscript published on 28 February 2019.

* Correspondence Author (s)

Sher Afghan Khan*, Department of Mechanical Engineering, International Islamic University Malaysia.

M. Mohiuddin Department of Mechanical Engineering, International Islamic University Malaysia.

Ahmad Saleel C. Dept. of Mech. Engineering, King Khalid University, Abha, Saudi Arabia.

Fharukh G. M. Research Scholar Department of Mechanical Engineering, Bearys Institute of Technology, Mangalore, Karnataka, India.

Assistant Professor Department of Mechanical Engineering, Government Engineering College, Huvinahadagali, Karnataka, India.

© The Authors. Published by Blue Eyes Intelligence Engineering and Sciences Publication (BEIESP). This is an [open access](https://creativecommons.org/licenses/by-nc-nd/4.0/) article under the CC-BY-NC-ND license <http://creativecommons.org/licenses/by-nc-nd/4.0/>.

II. LITERATURE REVIEW

In Ahmed and Khan [5], the capability of flow regulations to control the base pressure of a suddenly expanded pipe is evaluated. From the data obtained, it is found that there is no considerable gain in the base pressure region in low NPR, but for higher NPR's, noteworthy variations in the base pressure region can be identified. Thus it can be concluded that significant role is played by NPR to resolve the base pressure magnitude and control capability of flow regulations.

Pathan, Khan, and Dabeer [6] discussed the consequence of Mach numbers on velocity distribution for varying area ratio and NPR from cd nozzle to abruptly expanded the circular pipe of substantial cross-sectional area. From the obtained data, it can be identified in such case the expanded pipe is greatly influenced by Mach numbers, NPR and Area ratio. Besides, for larger values of NPR, the flow is seen to be under-expanded, and waves are found. This tendency is found until the under-expansion level is decreased, and the pressure equals to the back pressure.

In an experimental analysis performed by Saleel, Baig, and Khan [9], airflow from cd axisymmetric nozzles is abruptly expanded into a circular pipe of greater cross-sectional area. The experimental data that is obtained suggests that for NPR 3, no noteworthy gain is present and so the control utilized with the microjets is not useful here. However, for NPR 3, the experimental data suggests notable changes in base pressure for every area ratios.

Another experiment was conducted in Quadros, Khan, and Antony [7], where base pressure changes are identified from an abruptly expanded axisymmetric transit. From this Taguchi design of experiments, the enlargement length to diameter ratio can be found resulting in increasing or decreasing pressure at the base. Besides, from the experiment conducted, it is found that the reattachment length increases with the increasing of Mach numbers. The reason behind it is the strong vortex at the base, and thus a stronger suction is found at the base.

In work done by Khan and Aabid [1], the efficiencies of microjets were evaluated to control base pressure in the abruptly expanded planar pipe. The data suggests that the total pressure is changing considerably from inlet to outlet. Moreover, with the decrease of pressure, velocity is seen to increase. The dissimilarity of pressure inlet to the pressure outlet is also noticed by reviewing the Mach number.

III. METHODOLOGY

A CFD based study should follow several steps in order to give acceptable results, and a minor mistake can lead to a considerable amount of deviation from the actual results. In order for the process to proceed, the geometry of the model is created which is followed by the mesh generation. The physics and fluid properties are selected followed by the specification of boundary conditions. Initialization and solution control is done, and the convergence is monitored. In order to verify and validate the results, post-processing is done [12]. The Mach numbers of this experimental simulation are based on nozzle exit Mach number. Three models are used in this experiment corresponding to the different Mach numbers. From CFD experiments and

results, the calibrated Mach numbers differ from the design Mach numbers. Table I shows the comparison between the design and the calibrated Mach numbers.

Table I
Comparison of Design and Calibrated Mach numbers

	Design Mach Number	Calibrated Mach Number
Inlet Diameter (Di)	1.7	1.87
Throat Diameter (Dt)	2.4	2.20
Exit Diameter (de)	2.7	2.58

The calibrated Mach numbers were used in this simulation. The throat areas for the specific models are different in order to achieve different nozzle exit Mach numbers. The geometries of the models shown in Figure 1 and Table I were taken from [13]. The specifications of the models which were used for the specific Mach numbers are given in Table II.

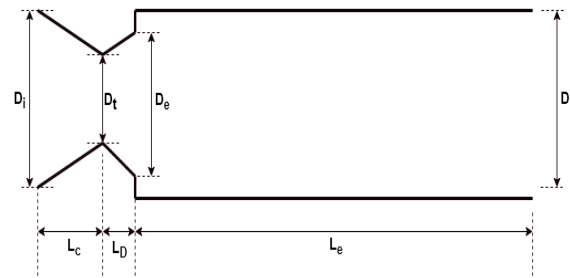


Fig. 1. The geometry of the CD Nozzle

Table II Dimensions of the CD nozzle for different Mach numbers

	Model 1 (Mach-1.87)	Model 2 (Mach-2.2)	Model 3 (mach-2.58)
Inlet Diameter (Di)	28.72	26.523	25.677
Throat Diameter (Dt)	8.648	6.45	5.605
Exit Diameter (De)	10	10	10
Extended diameter (D)	16	16	16
Convergent Length (Lc)	35	35	35
Divergent length (Ld)	12.926	16.88	20.907
Extended length (Le)	160	160	160

The nozzle geometry is done by the 2D planar body in ANSYS Workbench from the dimensions given in Table 1. Figure 2 shows the 2D planar finite element model for a particular design Mach number used. Separate geometries were constructed for each of the design Mach numbers.



Fig. 2. 2D Model made in ANSYS

The meshing of the geometry was then carried out. The meshing of geometry is one of the most discussed topics in CFD. The accuracy and the stability are determined from the meshing, and the denser the mesh is, the higher is the stability and accuracy of the computation.

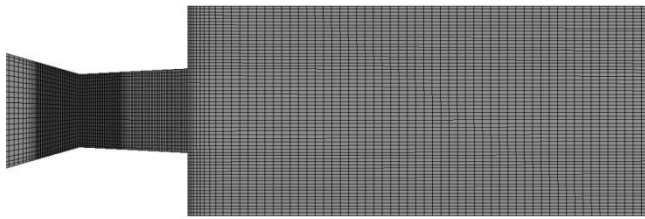


Fig. 3. The meshing of the Nozzle

For the boundary condition specifications, the inlet was specified as pressure inlet, the outlet was specified as pressure outlet, the wall was assigned as a solid wall. Pressure inlet boundary condition was used to define the fluid pressure at flow inlets. The inlet pressure for every case is calculated according to NPR. The outlet pressure for every case is considered as one atmospheric pressure. 3, 5, 7, 9, 11 are the Nozzle Pressure Ratios used for the analysis. Wall boundary condition was used as a stationary wall and no-slip condition. For this study, the Standard $k-\omega$ model is used with the energy equation.

IV. RESULTS AND DISCUSSION

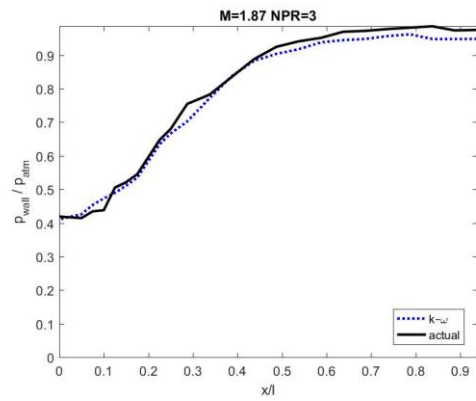
Effects of the Nozzle Pressure Ratio, Nozzle Exit Mach Number on the total pressure across the duct, velocity across the duct. Moreover, the base pressure is examined in this section. A combination of three nozzle exit Mach numbers of 1.87, 2.2, 2.58 and five NPR of 3,5,7,9, and 11 is used to identify the effects. CFD simulation using ANSYS Fluent was carried out to obtain the necessary plots and contours.

Validation of the Results

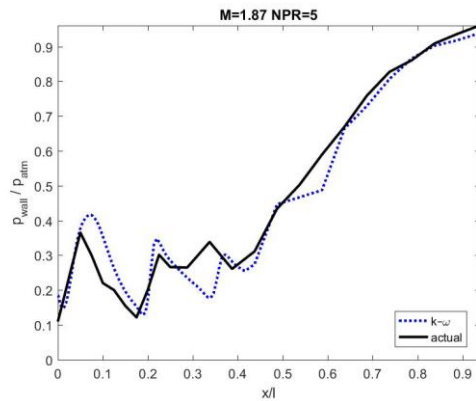
Upon plotting the experimental non-dimensional values measured by Baig et al. [12] and Standard $k-\omega$ model, CFD simulation results for all 15 cases are as shown in Figure 4. Figures 4(a) - 4(e) are for Mach no. 1.87, Figures 4(f) - 4(j) are for Mach no. 2.2 and Figures 4(k) - 4(o) are for 2.58. It can be observed from Figure 4 that the two curves are almost identical with an acceptable error percentage. Table 2 shows the comparison for $M=2.58$ and $NPR=11$, and as seen the margin for error is acceptable.

Table II
Comparison between Experimental and Simulated Static Pressures

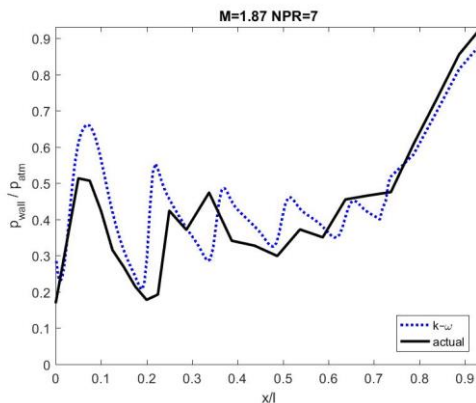
Position	Experimental Static Pressure (Pa)	Simulated Static Pressure (Pa)
The beginning of the duct	-70927.5	-55728.75
End of the duct	-30385.5	-30397.5



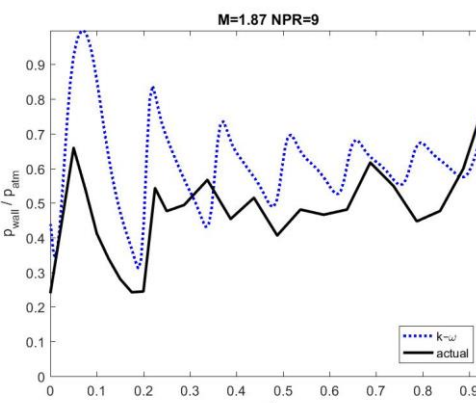
(a)



(b)

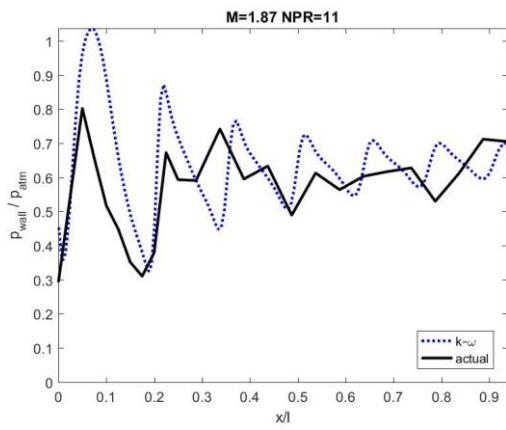


(c)

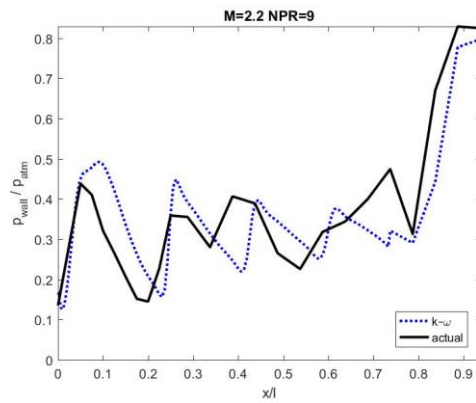


(d)

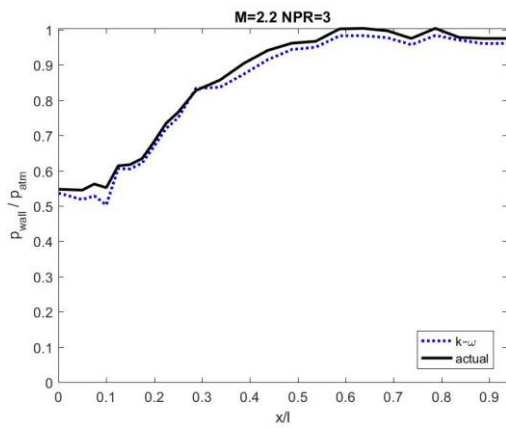
Investigation of the Effects of Nozzle Exit Mach Number and Nozzle Pressure Ratio on Axisymmetric Flow through Suddenly Expanded Nozzles



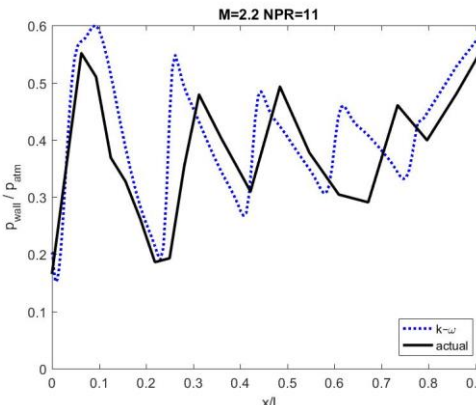
(e)



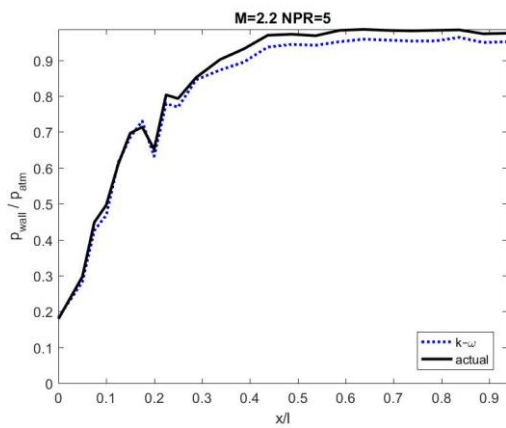
(i)



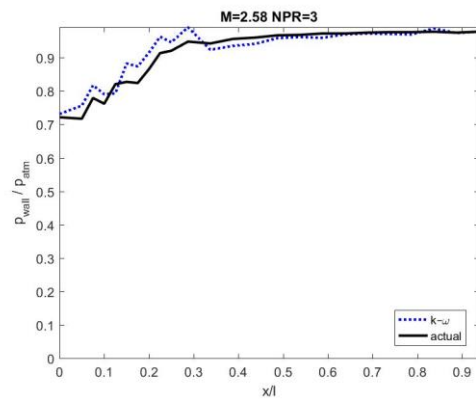
(f)



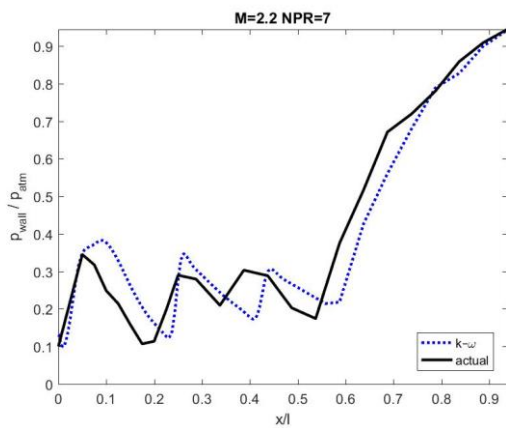
(j)



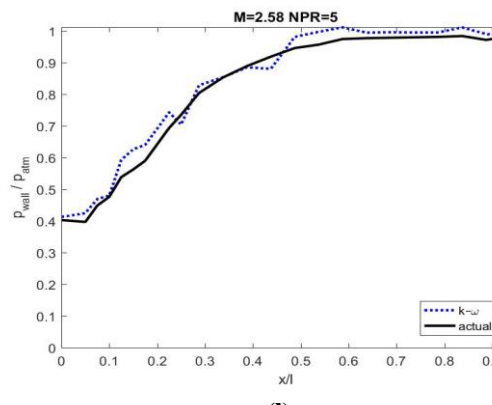
(g)



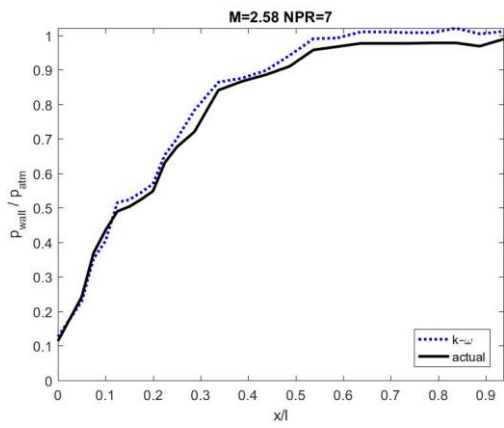
(k)



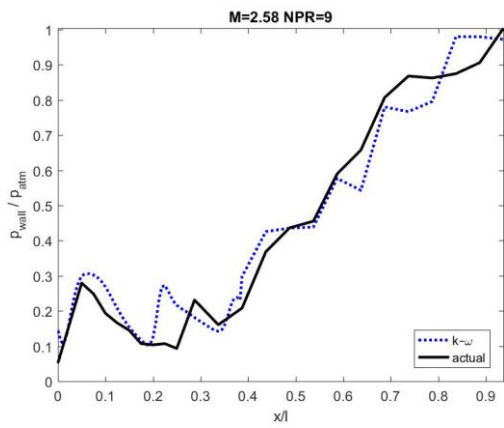
(h)



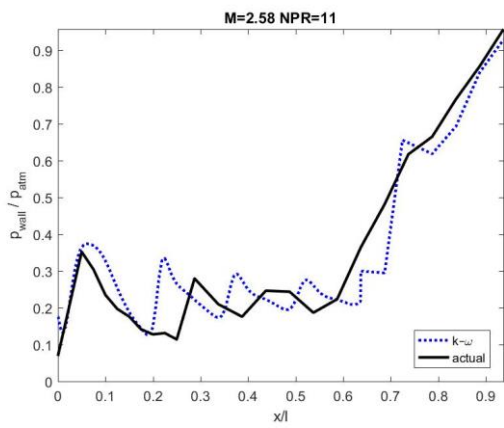
(l)



(m)



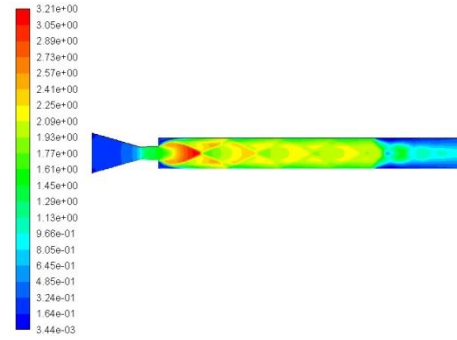
(n)



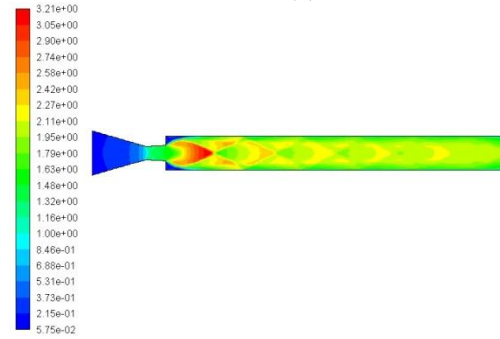
(o)

Fig. 4. Non-dimensional wall pressure vs. Non-dimensional axial position comparison for (a) M = 1.87, NPR = 3; (b) M = 1.87, NPR = 5; (c) M = 1.87, NPR = 7; (d) M = 1.87, NPR = 9; (e) M = 1.87, NPR = 11; (f) M = 2.2, NPR = 3; (g) M = 2.2, NPR = 5; (h) M = 2.2, NPR = 7; (i) M = 2.2, NPR = 9; (j) M = 2.2, NPR = 11; (k) M = 2.58, NPR = 3; (l) M = 2.58, NPR = 5; (m) M = 2.58, NPR = 7; (n) M = 2.58, NPR = 9; (o) M = 2.58, NPR = 11

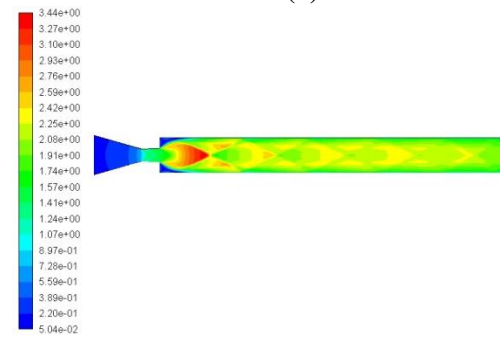
Now, in Figures 5 and 6, the Mach number contours and Total Pressure contours are shown respectively. Figures 5(a) - 5(e) are for Mach no. 1.87, Figures 5(f) - 5(j) are for Mach no. 2.2 and Figures 5(k) - 5(o) are for Mach 2.58. Similarly, Figures 6(a) - 6(e) are for Mach no. 1.87, Figures 6(f) - 6(j) are for Mach no. 2.2 and Figures 6(k) - 6(o) are for Mach number 2.58.



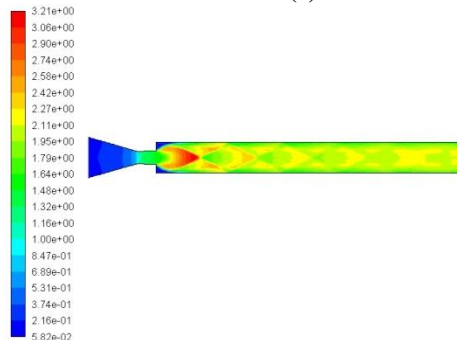
(a)



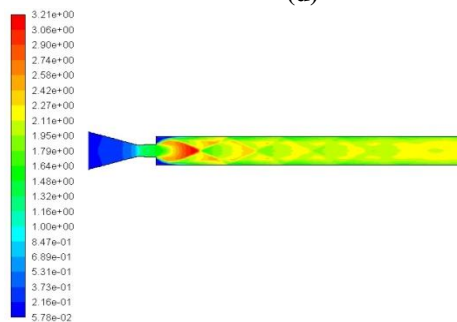
(b)



(c)



(d)



(e)

Investigation of the Effects of Nozzle Exit Mach Number and Nozzle Pressure Ratio on Axisymmetric Flow through Suddenly Expanded Nozzles

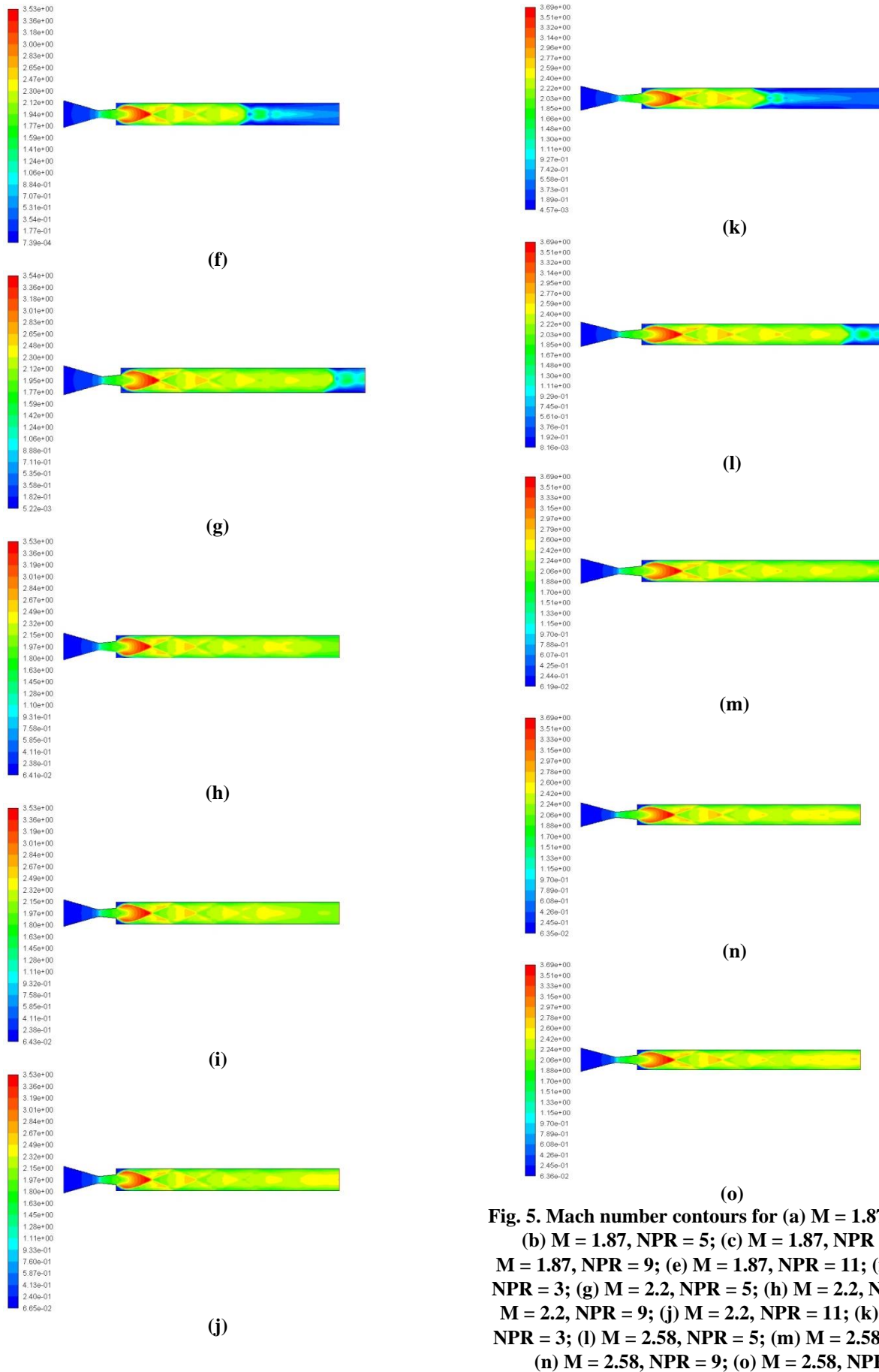
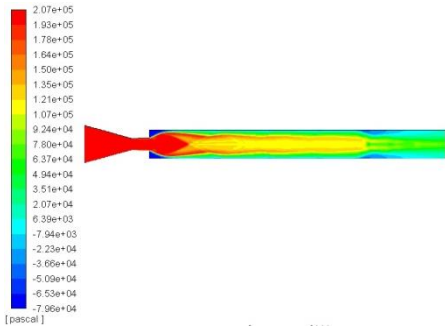
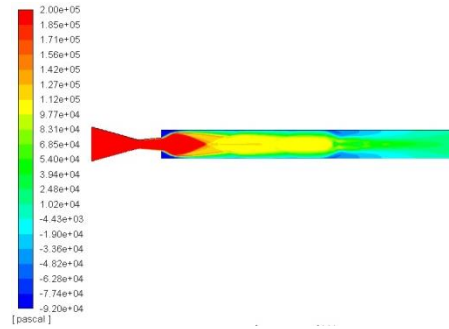


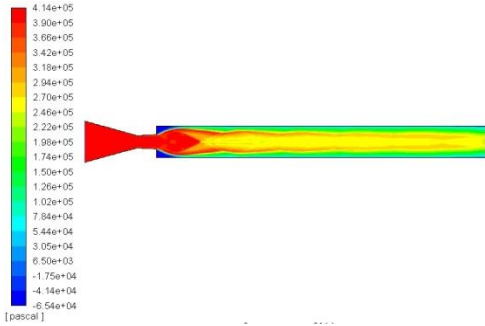
Fig. 5. Mach number contours for (a) $M = 1.87$, $NPR = 3$; (b) $M = 1.87$, $NPR = 5$; (c) $M = 1.87$, $NPR = 7$; (d) $M = 1.87$, $NPR = 9$; (e) $M = 1.87$, $NPR = 11$; (f) $M = 2.2$, $NPR = 3$; (g) $M = 2.2$, $NPR = 5$; (h) $M = 2.2$, $NPR = 7$; (i) $M = 2.2$, $NPR = 9$; (j) $M = 2.2$, $NPR = 11$; (k) $M = 2.58$, $NPR = 3$; (l) $M = 2.58$, $NPR = 5$; (m) $M = 2.58$, $NPR = 7$; (n) $M = 2.58$, $NPR = 9$; (o) $M = 2.58$, $NPR = 11$



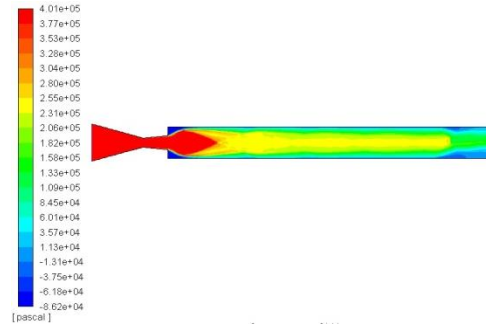
(a)



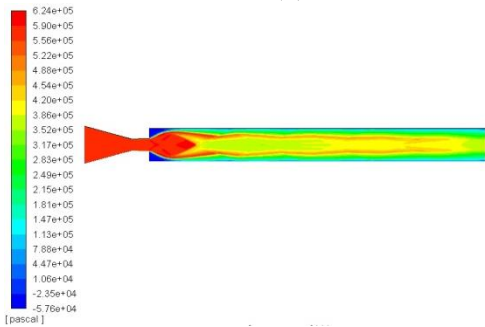
(f)



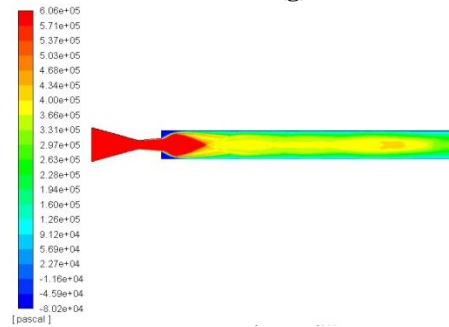
(b)



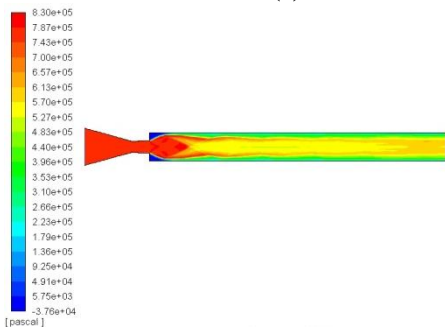
(g)



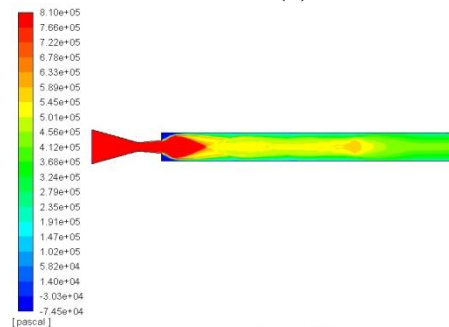
(c)



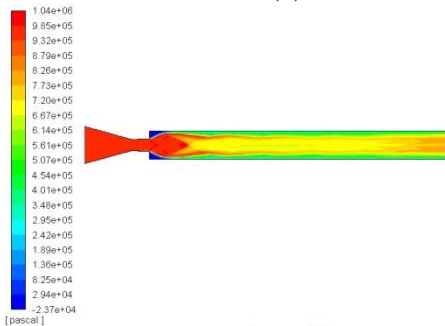
(h)



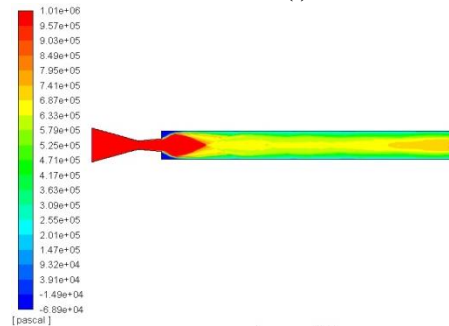
(d)



(i)



(e)



(j)

Investigation of the Effects of Nozzle Exit Mach Number and Nozzle Pressure Ratio on Axisymmetric Flow through Suddenly Expanded Nozzles

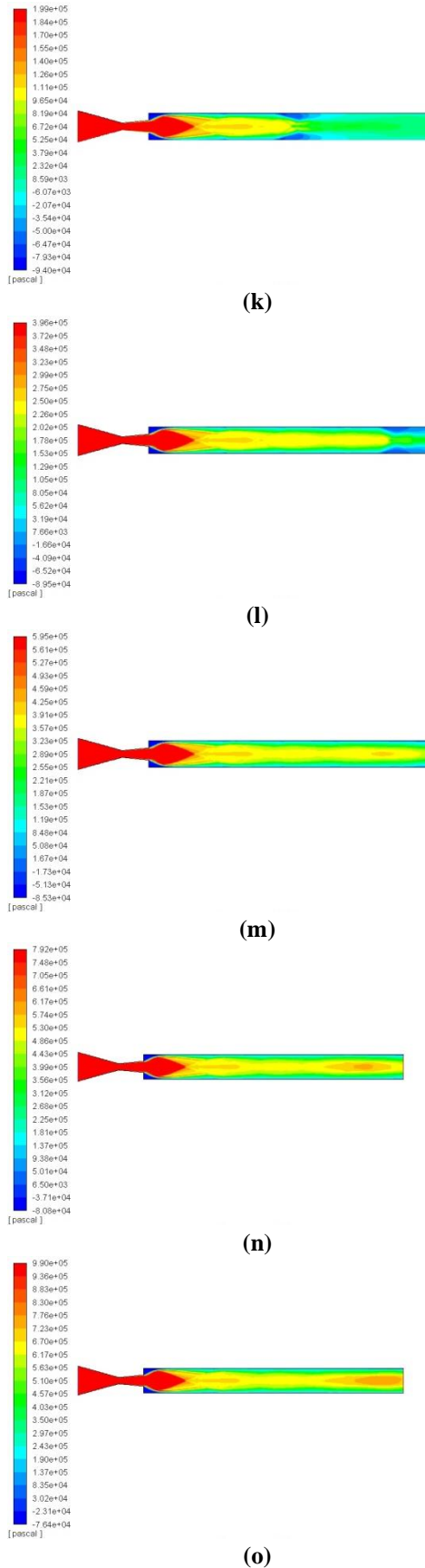


Fig. 6. Total Pressure Contours for (a) $M=1.87$, $NPR=3$; (b) $M=1.87$, $NPR=5$; (c) $M=1.87$, $NPR=7$; (d) $M=1.87$, $NPR=9$; (e) $M=1.87$, $NPR=11$; (f) $M=2.2$, $NPR=3$; (g) $M=2.2$, $NPR=5$; (h) $M=2.2$, $NPR=7$; (i) $M=2.2$, $NPR=9$; (j) $M=2.2$, $NPR=11$; (k) $M=2.58$, $NPR=3$; (l) $M=2.58$, $NPR=5$; (m) $M=2.58$, $NPR=7$; (n) $M=2.58$, $NPR=9$; (o) $M=2.58$, $NPR=11$

Effect of NPR on the total pressure across the duct

The contours for total pressure which in theory is the sum of static and dynamic pressure are all shown in Figure 6. The first model which gives a Nozzle exit Mach number of 1.87. Upon observing the contours for 1.87, as the NPR increases, the pressure at the inlet increases. It is right by its very definition. Also, for every case, there is a small area of low pressure (depicted in blue) created as soon as the flow is suddenly expanded.

Additionally, as the NPR increases, the pressure differential between the duct exit pressure and the atmospheric pressure is increased. That shows that at NPR 3 the flow might leave the duct ideally or over-expanded. However, for other cases, with an increase in NPR, the flow will become more and more under-expanded.

Effect of Nozzle Exit Mach Number on the total pressure across the duct

Figure 6(a), 6(f) and 6(k) depict the total pressure contours drawn for nozzle exit Mach numbers of 1.87, 2.2 and 2.58 for a fixed NPR of 3. These Mach numbers were achieved by creating different models in ANSYS Fluent as per the specifications mentioned in the previous section. To accurately spot the effects of Nozzle Exit Mach number, results for a fixed NPR of 3 are chosen. Upon inspection, flow through the duct for all the cases is mainly higher than the atmospheric pressure, except for the low-pressure suction zones created. All cases display the creation of two suction zones along the axial length of the duct. One is due to the sudden expansion, and another is due to flow separation as the inlet pressure, in this case, is lower. However, as observed the second suction area moves farther from the duct exit as the Mach number increases.

Now, for a higher nozzle pressure ratio of 11, as observed from Figures 6(e), 6(j), 6(o), no suction zones apart from the one after the sudden expansion is created. Small pockets of high pressure are created as the Mach number increases.

Effect of NPR on the velocity across the duct

In Figure 5, Mach number contours for different NPR's and Nozzle Exit Mach numbers are displayed. With an increase in NPR, the magnitude of the velocity at the exit of the duct keeps increasing as observed for a fixed NPR of 3 from Figures 5(a), 5(f), and 5(k); and for a fixed NPR of 11 from Figures 5(e), 5(j), and 5(o). For NPR 3, the flow exits with a Mach number of about 0.85 whereas, for NPR 11, the flow leaves with a Mach number of around 2.2. Which, signifies that with an increase in NPR, stronger oblique shockwaves are formed.

Effect of Nozzle Exit Mach Number on the velocity across the duct

Just like the total pressure, velocity across the duct returns to subsonic faster as the Mach number at the nozzle exit increases. For instance at a distance from the nozzle $x=110$ mm, for the first case in Figure 5(a), the flow is still supersonic, whereas for the last case in Figure 5(j) the flow has already become subsonic.

For higher NPR's (9 in this case), the effect is similar to that of the lower NPR's as discussed above, since the strength of the oblique shockwaves keeps diminishing as the Mach number at the nozzle increases. The flow does not become subsonic because oblique shockwaves have higher energy for a higher NPR, but the effect can be observed in Figures 5(d), 5(i), 5(n).

Effect of Nozzle Exit Mach Number and NPR on base pressure

The simulated data for base pressure is plotted for all the cases in Figure 7. As seen, an increase in NPR increases the base pressure. Furthermore, an increase in the nozzle exit Mach number reduces the base pressure magnitude. This is important to note that since base pressure is the primary source of drag in a suddenly expanded duct. In order to minimize this base drag, an active or passive method of drag control may be applied.

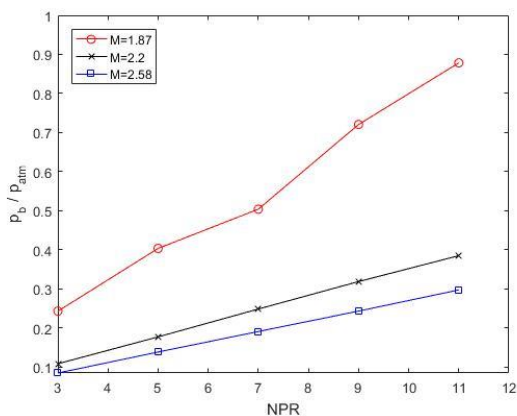


Fig. 7. Simulated Non-dimensional base pressure vs. NPR for different Mach numbers

V. CONCLUSIONS

All the simulations in this analysis were run using the standard k- ω model. The simulated data was verified with experimental results, and many essential observations were collected. The first of which is that as the NPR increases, the total pressure at the exit of the duct increases. This is particularly important as the flow becomes more and more under-expanded with an increase in NPR. Secondly, the increase in NPR also strengthens the oblique shockwaves across the duct, and the flow becomes subsonic later. Nozzle exit Mach number also influences the total pressure and velocity across the duct. Increasing Nozzle exit Mach number decreases the flows ability to remain attached at the duct surfaces. Also, the flow velocity returns to subsonic earlier across the duct as the Mach number at the nozzle exit increases. Lastly, increasing NPR increases the base pressure whereas increasing nozzle exit Mach number, decreases it. For future work, the effect of NPR and Nozzle Exit Mach number on the reattachment length can be found.

REFERENCES

1. S. A. Khan and A. Aabid, "CFD analysis of Cd nozzle and effect of Nozzle Pressure Ratio on pressure and velocity for suddenly expanded flows," Int. J. Mech. Prod. Eng. Res. Dev., vol. 8, no. June, pp. 1147–1158, 2018.

2. D. K. Walters, S. Bhushan, E. Merzari, and A. Obabko, "Fedsm2014-22055 Spectral Element Solver Nek5000," pp. 1–8, 2014.

3. L. O. Amoudry, "Extension of k- ω turbulence closure to two-phase sediment transport modelling: Application to oscillatory sheet flows," Adv. Water Resour., vol. 72, pp. 110–121, 2014.

4. V. Sethuraman and S. A. Khan, "Base Pressure Control using Micro-jets in Supersonic Flow Regimes," Int. J. Aviat. Aeronaut. Aerosp., no. February, 2018.

5. F. Ahmed and S. A. Khan, "Investigation of efficacy of low length-to-diameter ratio and nozzle pressure ratio on base pressure in an abruptly expanded flow," MATEC Web Conf., vol. 172, no. January, p. 1004, 2018.

6. K. A. Pathan, S. A. Khan, and P. S. Dabeer, "CFD analysis of effect of Mach number, area ratio and nozzle pressure ratio on velocity for suddenly expanded flows," 2017 2nd Int. Conf. Converg. Technol. I2CT 2017, vol. 2017–Janua, no. June 2018, pp. 1104–1110, 2017.

7. J. D. Quadros, S. A. Khan, and A. J. Antony, "Investigation of effect of process parameters on suddenly Expanded flows through an axisymmetric nozzle for different Mach Numbers using Design of Experiments," IOP Conf. Ser. Mater. Sci. Eng., vol. 184, no. April, p. 12005, 2017.

8. K. A. Pathan, S. A. Khan, and P. S. Dabeer, "CFD analysis of effect of area ratio on suddenly expanded flows," 2017 2nd Int. Conf. Converg. Technol. I2CT 2017, vol. 2017–Janua, no. June 2018, pp. 1192–1198, 2017.

9. A. Saleel, M. A. Ali Baig, and S. A. Khan, "Experimental Investigation of the Base Flow and Base Pressure of Sudden Expansion Nozzle," IOP Conf. Ser. Mater. Sci. Eng., vol. 370, no. May, p. 12052, 2018.

10. M. Asadullah, S. A. Khan, W. Asrar, and E. Sulaeman, "Passive control of base pressure with static cylinder at supersonic flow," IOP Conf. Ser. Mater. Sci. Eng., vol. 370, no. May, p. 12050, 2018.

11. M. Bashir and S. A. Khan, "Investigation on the Prominence of Abrupt Expansion on the Base Pressure of an Axi-Symmetric Body," no. December, pp. 2–7, 2017.

12. Tu, J., Yeoh, G. H., & Liu, C. (2013). Computational fluid dynamics: a practical approach Elsevier/Butterworth Heinemann.

13. M. A. A. Baig, S. A. Khan, C. Ahmed Saleel, and E. Rathakrishnan, "Control of base flows with micro jet for area ratio of 6.25," ARPN J. Eng. Appl. Sci., vol. 7, no. 8, pp. 992–1002, 2012.